THE JOURNAL OF PHYSICAL CHEMISTRY A

pubs.acs.org/JPCA Article

The Conformational Landscape, Internal Rotation, and Structure of 1,3,5-Trisilapentane using Broadband Rotational Spectroscopy and Quantum Chemical Calculations

Published as part of The Journal of Physical Chemistry virtual special issue "International Symposium on Molecular Spectroscopy".

Atef Jabri, Frank E. Marshall, William Raymond Neal Tonks, Reid E. Brenner, David J. Gillcrist, Charles J. Wurrey, Isabelle Kleiner, Gamil A. Guirgis, and G. S. Grubbs II*

Cite This: *J. Phys. Chem. A* 2020, 124, 3825−3835 Read Online

ACCESS | Metrics & More | Article Recommendations | Supporting Information

ABSTRACT: The rotational spectrum of 1,3,5-trisilapentane was observed on a chirped-pulse Fourier transform microwave spectrometer and is reported. During assignment, multiple conformations of the molecule were identified in the molecular beam. Prior quantum-chemical calculations performed on the molecule show that the identified spectra correspond to the lowest three calculated energetic structures. These structures are of C_2 (Conf.1), C_{2v} (Conf.2), and C_1 (Conf.3) symmetry, with relative energy ordering of Conf.1 < Conf.3 < Conf.2, which is in stark contrast to *n*-pentane and all known silicon-substituted *n*-pentane derivatives. This is found to most likely arise from the elongation of the Si−C bond and the size of the silicon atoms providing for the C_2 and C_1 structures relieving steric hindrance in comparison to that of the C_{2v}. In the C_{2v} and C_1 conformers, splitting in the spectra due to internal rotation of the $-SiH_3$ end groups of 1,3,5-trisilapentane was observed and determined. The C_{2v} equivalent V_3 values are 368.46(33) cm^{-1}, and the C_1V_3 values are 347.78(21) and 360.18(88) cm^{-1}, respectively. These barriers are compared to similar species in order to help verify their veracity and are determined to be accurate based on similar molecular silyl rotors.

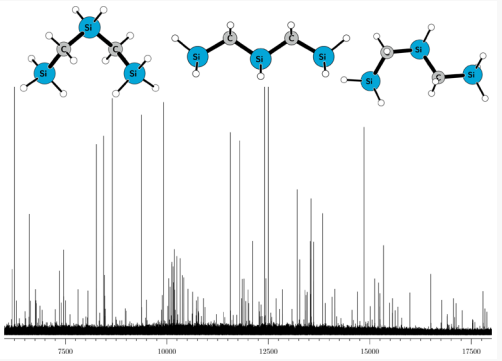

INTRODUCTION

Methyl rotor internal rotation is a topic that has been heavily studied for over 60 years.[1−6] Over the past 45+ years, the molecular structure and internal rotation dynamics of species with one or two $-SiH_3$ groups have been of significant interest.[1,4,7−19] This interest and area of study has been significantly driven from the differences in molecular structure upon substitution of a carbon atom by a silicon atom. The general elongation of the bond created from the Si substitution lowers torsional energy strain, providing more freedom for the $-SiH_3$ group to rotate. Experiments, however, with molecules like disilane $H_3Si\text{-}SiH_3$ show that this internal rotation is not necessarily as "free" (barrier height: 407 cm^{-1})[18,19] as one would expect when compared to silane compounds such as methylsilane CH_3SiH_3 (395 cm^{-1})[1] or silyl methyl ether CH_3OSiH_3 (385 cm^{-1}).[14] Since the barrier height for internal rotation in these species (disilane, methyl silane, and methyl silyl ether) results from a complex interplay of a number of factors—as discussed by Goodman[10]—it would take an exceedingly fortuitous and unlikely cancellation of these factors to yield free internal rotation in disilane. Furthermore, disilane gas-phase infrared vibrational spectra show no evidence of free internal rotation, and "Qualitatively, the structure of the ⊥ bands ν_7 and ν_8 for disilane resembles very closely that found for ethane, which has a sizable barrier to internal rotation."[7] All of these make further investigations on the role of the separation between the two rotors a very important area of study.

In addition to silyl internal rotation, the molecular structure of pentane and pentane derivatives has also been studied heavily with molecular spectroscopy approaches.[20−25] The torsional flexibility of the chained backbone in these molecules provides for a wide array of conformations, providing for a rich and intriguing conformational landscape. In the gas-phase microwave spectroscopy study of perfluoropentane, for example, this flexibility allows the fluorines in the molecule

Received: February 8, 2020
Revised: April 22, 2020
Published: April 23, 2020

https://dx.doi.org/10.1021/acs.jpca.0c01100
J. Phys. Chem. A 2020, 124, 3825−3835

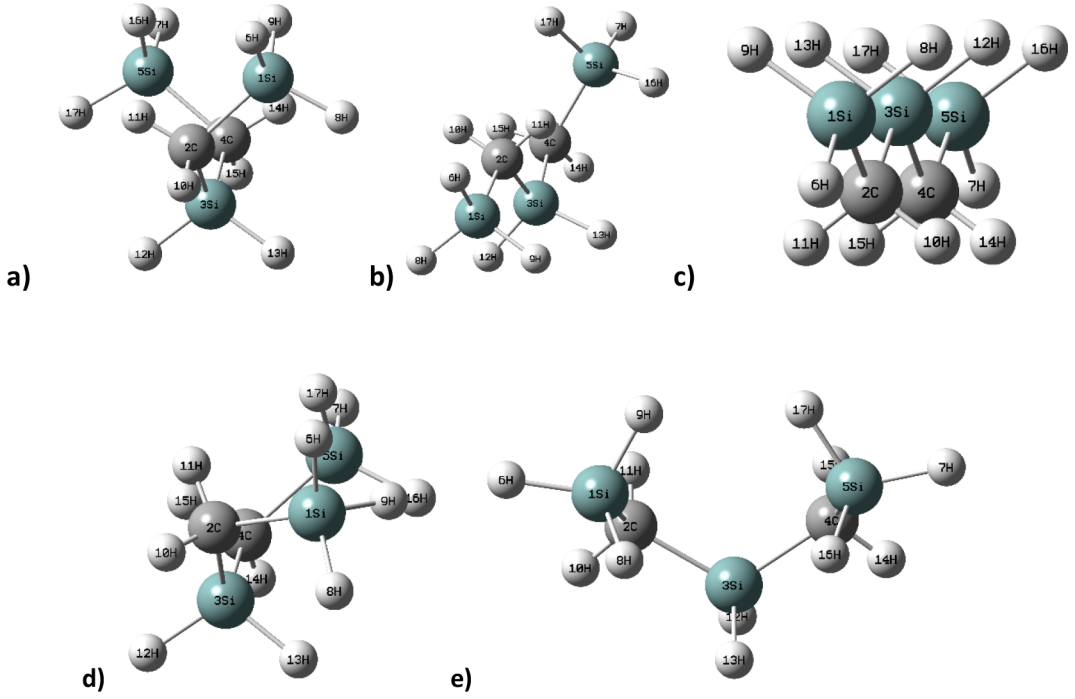

Figure 1. Five optimized geometries of 1,3,5-trisilapentane. The structures are presented in order to best show symmetry elements. The symmetries are (a) C_2, (b) C_1 (TG), (c) C_{2v}, (d) C_1 (GG′), and (e) C_s.

to be distributed in a spiral, providing C_2 symmetry rather than the C_{2v} symmetry of the hydrocarbon.[20]

This potentially rich conformational landscape, then, requires additional investigation, particularly in the case of substituting Si atoms due to Si-bond elongation. Previously, conformational stability studies of pentane and its silicon-substituted derivatives were performed using vibrational spectroscopy. In the case of *n*-pentane, various computational approaches[21,26−29] have identified five possible conformations, having the following symmetries: C_{2v} (*trans, trans* (TT)); C_1 (*trans, gauche* (TG)); C_2 (*gauche, gauche* (GG)); C_s (*gauche, gauche′* (GG′)); and a second C_1 form (*gauche, gauche′* (C_1 (GG′)), which has unusual dihedral angles of ∼65 and ca. −91°, in contrast to expected ∼60 or ∼180° values. Because of steric hindrance, however, the C_s (GG′) conformer is less stable and has been noted by Salam and Deleuze[27] as being "sterically forbidden." Each of these conformers for 1,3,5-trisilapentane is presented in Figure 1.

Evidence for all except the C_s species exist from the vibrational spectra of *n*-pentane in condensed phases (summarized by Mirkin and Krimm[21]) and from a gas-phase Raman spectrum obtained by Balabin.[29] Peaks that readily correspond to the predicted frequencies of the most intense Raman-active vibrations below 500 cm^{-1} of the C_2, C_{2v}, and the "regular" C_1 conformer have been confidently assigned. Additionally, a very weak peak near 360 cm^{-1} was also observed by Balabin,[29] and it is consistent with the predicted frequency for the most intense Raman-active vibration below 500 cm^{-1} for the "unusual" C_1 form. The relative weakness of this conformer's Raman band near 360 cm^{-1} is a result of its being, not surprisingly, notably higher in energy than the other three stable conformers of *n*-pentane and, thus, less abundant.

Experimentally, the enthalpy difference between the TT-TG conformers of *n*-pentane was determined to be 600 ± 100 cal mol^{-1} (209.9 ± 35 cm^{-1}), and the enthalpy difference between the GG-TG conformers was determined to be 670 ± 100 cal mol^{-1} (234 ± 35 cm^{-1}) with the TT conformer as the most stable conformer.[21] Interestingly, the authors found TT, TG, and GG conformers in the liquid and the solid state of the sample.[21] Similarly, one of the authors of this work also was involved in a liquid Raman study of the CCC bending region of *n*-pentane near 400 cm^{-1}, which found the TT conformer to be the most stable.[30] The TG conformer was found to be the second-lowest energy conformer at 164 ± 10 cm^{-1} above, in agreement with the Mirkin and Krimm work. Similar conformational stability patterns were observed for *n*-butylsilane ($SiH_3CH_2CH_2CH_2CH_3$) and diethylsilane ($CH_3CH_2SiH_2CH_2CH_3$). For both compounds only the TT form was observed in the crystalline solid form, whereas TT, TG, and GG conformers were observed in the liquid and the gaseous state of the sample.[22,23,31] In *n*-butylsilane, again one of the authors of this work was involved in determining that TT was the most stable species, followed by the TG conformer 227 ± 10 cm^{-1} higher in energy.[31] In the gas-phase electron diffraction study of 1,5-disilapentane the TT conformer was observed to be the most stable form.[24] The energy difference between the GG and TT forms was determined to be 1.0 kJ mol^{-1} (84 cm^{-1}), and the energy difference between the TG and GG forms was determined to be 2.8 kJ mol^{-1} (234 cm^{-1}), whereas according to theoretical calculations by using the SCF 3-21G*, SCF 6-21G*, and MP2 6-31G* basis sets, the conformational stability order was determined to be TT, TG, and then GG.[24] However, the authors had some doubt about the conformational stability of TG and GG forms, and no further study has been reported. Overall the second most stable conformer for pentane is TG, whereas for 1,5-disilapentane the second most stable conformer is GG.

For all of these reasons, we conducted and report the first microwave spectroscopic study on the molecule 1,3,5-trisilapentane. Microwave spectroscopy was used due to its unparalleled accuracy and precision in the determination of rotational constants, which speak directly to molecular

https://dx.doi.org/10.1021/acs.jpca.0c01100
J. Phys. Chem. A 2020, 124, 3825−3835

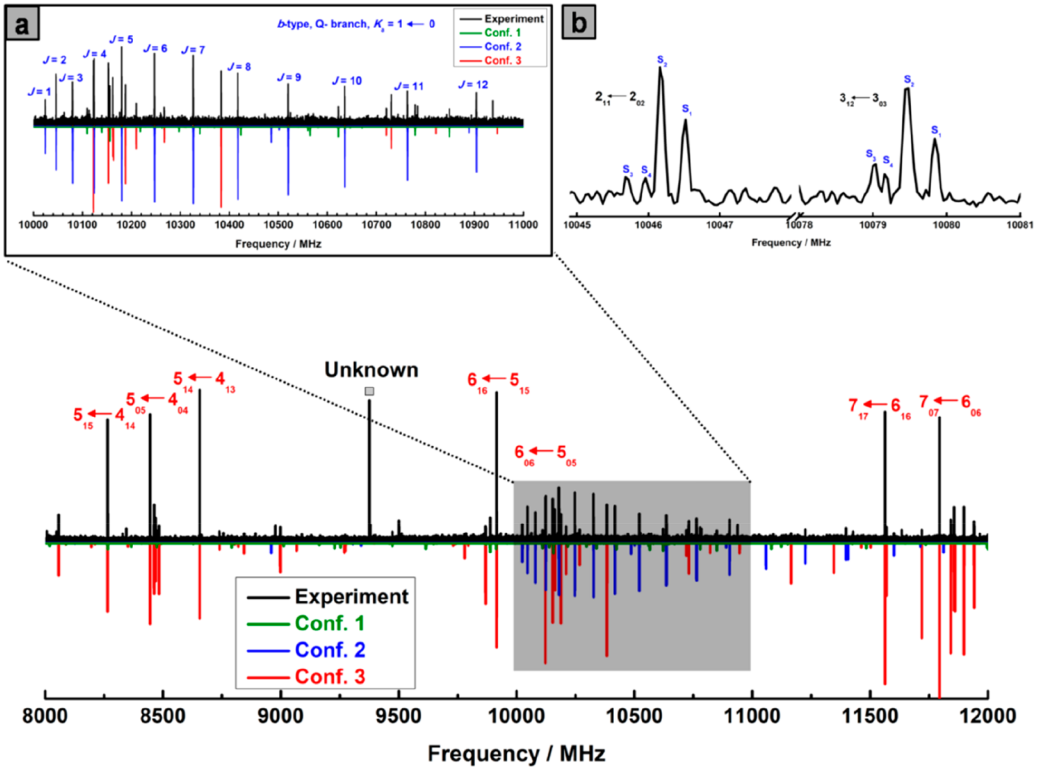

Figure 2. Comparison between experimental broadband rotational spectrum measured in the 8−12 GHz microwave region (black color) and simulated spectra of the three observed conformers of 1,3,5-trisilpentane. The "unknown" peak is believed to be background/manmade and not part of the rotational spectrum. (a) A portion of 1 GHz between 10 and 11 GHz highlighting the *b*-type Q-branch structure of Conf.2. (b) An expanded 40 MHz view showing the $2_{11} \leftarrow 2_{02}$ and $3_{12} \leftarrow 3_{03}$ transitions split into quadruplets due to equivalent internal rotation motions of the SiH_3 tops for Conf.2.

structure.[32] These studies are coupled with quantum-chemical calculations to eliminate the discrepancy in the literature with previously determined conformational landscapes, and the results are reported. In addition to this, microwave spectroscopy exhibits the resolution needed to observe internal rotation and determine accurate barrier heights to compare to similar silyl rotors.

EXPERIMENTAL SECTION

1,3,5-trisilapentane (TSP) was prepared by the Grignard reaction of 2 equiv of chloromethylsilane with powdered magnesium in dry diethyl ether and coupled with 1 equiv of dichlorodiethylsilane in dry diethyl ether. The product was filtered, and the ether was distilled off at reduced pressure. This product was reduced using lithium aluminum hydride in dry dibutylether, and TSP was obtained in a trap held at liquid nitrogen temperature. The identity of TSP was confirmed using infrared spectra of the gas and NMR spectra in deuterated chloroform.

The NMR spectra of the TSP product are as expected; ^{1}H NMR showed a multiplet at 0.01 ppm, a triplet at 3.64 ppm, and a second multiplet at 3.94 ppm. The ^{13}C NMR spectrum has one band at −15.44 ppm. The ^{29}Si spectrum shows two lines at −30.38 and −62.16 ppm. All of these values are consistent with the desired product and the absence of impurities.

After characterization of the synthesized TSP species, the sample was sent to the Missouri University of Science and Technology in order to obtain the rotational spectrum. As TSP is volatile, tanks containing a 3% gas mixture in Ar were prepared directly from the sample vial and repeated until no sample remained. The rotational spectrum was then obtained in the 6−18 GHz spectral region using a chirped-pulse Fourier transform microwave (CP-FTMW) spectrometer. This instrument has been detailed in the literature elsewhere.[33−36] The sample was introduced into the spectrometer at a backing gas pressure ∼1 atm above ambient (2 atm total) pressure from a pulsed supersonic nozzle (molecular beam). The chamber pressure, meanwhile, was held at 10^{-6} Torr. The spectra were obtained using 4 μs chirp widths at a pulse rate of 5 Hz, utilizing five 20 μs free induction decays (FIDs) per gas pulse. Spectra were collected in two 6 GHz bandwidth (6−12 and 12−18 GHz) regions using 610 000 FID averages per band. Typical line widths for completely resolved transitions range from 60 to 80 kHz with an uncertainty of 10 kHz in line centers. Example portions of the spectrum are presented in Figures 1 and 2.

QUANTUM-CHEMICAL CALCULATIONS

Given the conformational flexibility of the molecule, the first goal of the study was to identify the lowest-energy conformations of the molecule, as those would be the most probable species populated due to the molecular beam cooling. Quantum-chemical calculations were performed using the Gaussian09[37] and Gaussian16[38] programs. Since 1,3,5-trisilapentane is essentially *n*-pentane with silicon atoms substituted at every other position, it would not be unreasonable to expect that the possible conformations for both compounds would be similar.

https://dx.doi.org/10.1021/acs.jpca.0c01100
J. Phys. Chem. A 2020, 124, 3825−3835

Table 1. Zero-point Relative Energies and Predicted Spectroscopic Rotational Parameters[a]

Parameter	Unit	Conf.1 (C_2)	Conf.2 (C_{2v})	Conf.3 (C_1)
		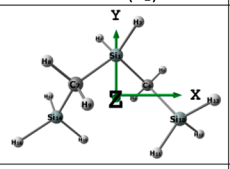	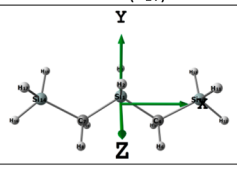	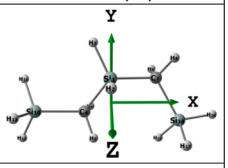
ΔE	cm^{-1}	0	79.7	102.1
ΔE	$kJ.Mol^{-1}$	0	0.95	1.22
A	MHz	3117	10950	5292
B	MHz	1248	694	886
C	MHz	1028	673	800
V_{3_1}	cm^{-1}	360	320	320
V_{3_2}	cm^{-1}	360	320	340
F_{0_1}	GHz	87.0	87.0	87.0
F_{0_2}	GHz	87.0	87.0	87.0
<(i,*a*)	°	59.8	150.1 [a]	61.3 [a]
<(i,*b*)	°	129.7	60.1 [a]	146.3 [a]
<(i,*c*)	°	54.4	90.0 [a]	73.8 [a]
$\|\mu_a\|$	Debye	0.00	0.00	0.62
$\|\mu_b\|$	Debye	0.20	1.40	0.00
$\|\mu_c\|$	Debye	0.00	0.00	0.67
μ_{total}	Debye	0.20	1.40	0.92
P_{aa} [b]	$uÅ^2$	367.2	716.72	553.1
P_{bb} [b]	$uÅ^2$	124.3	34.3	78.4
P_{cc} [b]	$uÅ^2$	37.86	11.8	17.1

[a]Zero-point relative energies and predicted spectroscopic rotational parameters for the three observed conformers of trisilapentane along with silyl rotor barriers to internal rotation parameters. All of these calculations were performed at the MP2/6-311++G(d,p) level of theory. [b]Fixed values for barrier height determination are from ab initio results. [c]Second planar moment values give the mass distribution along each principal axis; they are defined as $P_{ii} = 0.5(I_j + I_k - I_i)$, where I_j, I_k, and I_i are the moments of inertia about each molecular axis in question.[32]

Using B3LYP and MP2 (with full electron correlation) methods, then, ab initio calculations for 1,3,5-trisilapentane were performed using Gaussian09[37] with a variety of basis sets ranging from 6 to 31 G(d) to aug-cc-pVTZ. The goal was to identify all possible conformations and predict relative energy differences, rotational constants, and dipole moments. A full optimization (keyword "fopt") was performed, and each output file was examined to ensure each calculation did converge at the appropriate point group.

As expected, the computational results for 1,3,5-trisilapentane predict the same conformational symmetries as those for *n*-pentane, and the relative single-point (total) energies for each optimized structure are summarized in Tables S1 and S2 in the Supporting Information. For both B3LYP and MP2 methods, the C_s conformation is predicted to have the highest energy and produced one imaginary frequency. Therefore, the C_s conformation will not be discussed beyond these results. Surprisingly, the B3LYP and MP2 methods are contradictory in regard to the orderings of the four possible conformations: C_2 (GG), C_{2v} (TT), C_1 (TG), and C_1 (GG′). This inconsistency between B3LYP and MP2 was also reported by Salam and Deleuze[27] for high-level calculations of *n*-pentane.

From the B3LYP calculations, the C_{2v} form was predicted to be the most stable, followed by C_1 (TG), C_2, C_1 (GG′), and lastly C_s. Relative to C_2, the other four conformations produced consistent relative energies that appeared to be independent of the basis set used. The order of stability for 1,3,5-trisilapentane is congruent with the computational work done for *n*-pentane;[21,26−29] however, the relative energies of the four conformations for this study, with respect to C_{2v}, are lower in magnitude compared to previous studies of *n*-pentane. Such differences are likely a result of increased conformational flexibility, relative to *n*-pentane, due to longer bond lengths between C and Si atoms.

In contrast to the B3LYP method, MP2 calculations predicted the C_2 form as the most stable, followed by C_1 (TG), C_{2v}, and lastly C_1 (GG′). Relative energies between the other four conformations were sensitive to the basis set used. Additionally, the magnitude of the total energy for each conformation increased with added valence region functions, diffuse functions, and/or polarization functions. To address the inconsistency between high-level ab initio methods for 1,3,5-trisilapentane, experimental determination of enthalpy values between the four possible conformations is highly desirable to determine which method, either B3LYP or MP2, correctly predicts the order of conformational stability and to what, if any, degree of accuracy.

Geometry optimizations for the zero-point structures for the lowest three conformers of the MP2 calculations were performed at the MP2/6-311++G(d,p) level. The results of these quantum-chemical calculations, along with structural images of these calculations, are presented in Table 1. The new approach and level provided a slightly different conformational energy landscape from the original approach. C_2 was still the lowest energy (set to 0 cm^{-1}), but the C_{2v} structure was slightly lower in energy (79.7 cm^{-1}) than the C_1 structure (102.1 cm^{-1}). Only these three conformations were observed experimentally, and, as these structures were used in the fitting, the conformers are labeled Conf.1, Conf.2, and Conf.3 for the rest of the text with C_2 being Conf. 1, C_{2v} corresponding to Conf.2, and C_1 corresponding to Conf.3. Because only these species were experimentally observed, no further geometry optimizations for the zero-point energy structures of the C_1 (GG′) or C_s were undertaken. The

https://dx.doi.org/10.1021/acs.jpca.0c01100
J. Phys. Chem. A 2020, 124, 3825−3835

Table 2. Determined Spectroscopic Parameters of 1,3,5-Trisilapentane

		Conf.1	Conf.2		Conf.3	
		FIT 1	FIT 2	FIT 3	FIT 4	FIT 5
parameter	unit	SPFIT	SPFIT	XIAM	SPFIT	XIAM
A	MHz	3196.3878(22)[a]	10 711.3925(48)	10 710.8507(56)	5400.8951(97)	5400.8319(88)
B	MHz	1243.9778(11)	709.1641(16)	709.1833(14)	885.55704(40)	885.56831(32)
C	MHz	1033.56730(80)	687.0354(15)	687.0202(11)	807.38396(40)	807.37124(32)
D_J	kHz	1.3138(95)			0.3017(24)	0.2993(17)
D_K	kHz	20.89(41)			43.47(2.00)	51.63(1.79)
D_{JK}	kHz	−8.429(70)			−5.6710(96)	−5.6731(93)
d_j	kHz	0.4022(52)			−0.07479(50)	−0.07519(44)
d_k	kHz			0.159(32)	−0.00319(37)	−0.00258(31)
V_{3_1}	cm^{-1}			368.46(33)		347.78(21)
V_{3_2}	cm^{-1}			368.46(33)		360.18(88)
N[b]		26	16	53	79	336
rms[c]	kHz	10.8	12.4	14.7	11.3	23.0
P_{aa}[d]	uÅ^2	368.55840(28)	700.5264(12)	700.52371(92)	551.53181(22)	551.53257(18)
P_{bb}[d]	uÅ^2	120.40735(28)	35.0674(12)	35.08641(92)	74.41449(22)	74.42360(18)
P_{cc}[d]	uÅ^2	37.70207(28)	12.1140(12)	12.09743(92)	19.15870(22)	19.15069(18)

[a]Numbers in parentheses are the 1σ uncertainties of the measurement (67% confidence interval). [b]Number of measured/assigned transitions for each conformer. [c]The rms error is the microwave error defined as $\sqrt{\sum (\text{obs} - \text{calc})^2/N}$. [d]Second planar moment values give the mass distribution along each principal axis; they are defined as $P_{ii} = 0.5(I_j + I_k - I_i)$, where I_j, I_k, and I_i are the moments of inertia about each molecular axis in question.[32]

rotational constants provided from these geometry optimizations show, quantitatively, the very different nuclear positioning with respect to the principal axis system shown in Figure 1 and in Table 1. To further quantify this, second moments were calculated from the predicted rotational constants. As demonstrated by their P_{cc} values, Conf.2 and Conf.3 have very little mass out of the *ab* plane, while Conf.1 has much more of the heavy atom backbone out of the *ab* plane. Given the very small predicted energy differences of the conformers, the dipole moments would also play a large role in the observed intensity and transition types observed in the spectra. Conf.2 and Conf.3 were substantially more polar with calculated overall dipoles of 1.40 and 0.92 D, respectively, compared to 0.20 D for Conf.1.

After geometry optimizations were performed, the barriers to internal rotation for each $-SiH_3$ rotor were calculated, using potential energy scans obtained from the zero-point geometry optimizations at the MP2/6-311++G(d,p) level of theory. This resulted in six calculated barriers. The calculated barriers provide evidence of what would be expected given the predicted symmetries of the molecule. Both Conf.1 and Conf.2 have a pair of equivalent $-SiH_3$ rotors with V_3 = 356 cm^{-1} and V_3 = 320 cm^{-1}, respectively, while Conf.3 is predicted to have two inequivalent rotors with V_3 of the first being 320 cm^{-1} and V_3 of the other being 340 cm^{-1}. In the event all conformers were observed, then, the likelihood of observing splitting due to internal rotation in the molecule should be Conf.2 > Conf.3 > Conf.1.

RESULTS AND ANALYSIS

As expected from the quantum-chemical calculations, the resulting CP-FTMW spectrum was rich in transitions. In some regions, rather dense spectroscopic structures were observed with some of the rotational transitions split into three to five components having spacings ranging from 150 to 500 kHz. The conformational search and barrier height calculations, described in the quantum-chemical calculations, explain most of this, as the barrier height is low enough to possibly observe internal rotation, and the separations in conformational energies should provide significant population of more than one conformation in the molecular beam.

Pure Rotation Analysis. Although not predicted to be the lowest-energy conformer using MP2, Conf.2 had the largest dipole moment at 1.4 D, which was also predicted to lie along the *b*-axis, meaning only *b*-type transitions would be expected, simplifying the search. From the quantum-chemical calculations, the pure rotation constants for Conf.2 were predicted to be A = 10 950 MHz, B = 694 MHz, and C = 673 MHz (see Table 1). From this, we used Pickett's SPFIT/SPCAT program suite[39] to predict a rigid rotor spectrum using the pure rotational constants cited above. A typical *b*- type, *Q*-branch structure corresponding to $K_a = 1 \leftarrow 0$ was identified straightforwardly as shown in Figure 2a in blue color. Some *b*-type, *R*-branch transitions were also assigned, allowing an accurate determination of the A, B, and C parameters, at the kilohertz level, in a global fit of 16 lines converging with a root-mean-square (rms) deviation of 12.4 kHz (FIT 2 of Table 2). All fits are provided in the Supporting Information.

After discarding these 16 rotational signatures from our experimental spectrum, we then focused on the next highest intensity spectrum. This turned out to be Conf.3 of Table 1, which has the next largest predicted dipole moment (0.92 D) with components in the *a*- and *c*-directions ($|\mu_a|$ = 0.63 D, $|\mu_c|$ = 0.67 D).The *a*-type transitions corresponding to *R*-branch $(J + 1)_{K_a, (J+1)} \leftarrow J_{K_a, J}$ with J = 4, 5, or 6 and K_a = 0 or 1 (Figure 2, red color) were targeted first. Note that (and as Figure 2 shows), although these spectra arise from the same molecule, the difference in both conformation and transition type provide for very different asymmetric rotor patterns, simplifying spectral assignment. Then, we completed the assignments of the remaining *R*- and *Q*-branch, *c*-type pure rotation spectra of Conf.3. In total, we identified 79 lines converging with a root-mean-square deviation of 11.3 kHz (FIT 4 of Table 2). At this stage of analysis, Pickett's SPFIT/

https://dx.doi.org/10.1021/acs.jpca.0c01100
J. Phys. Chem. A 2020, 124, 3825−3835

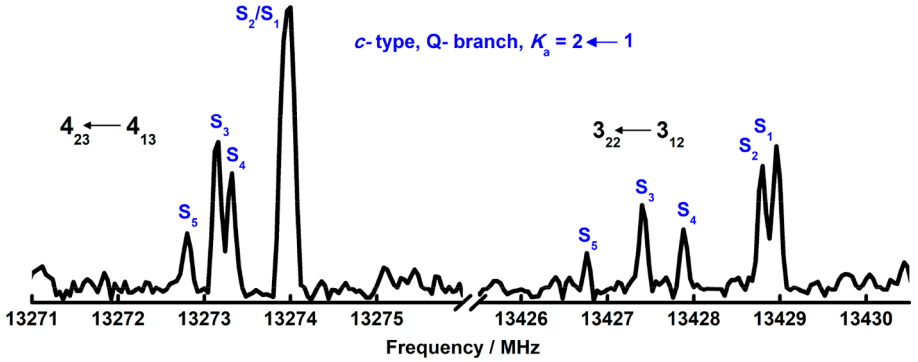

Figure 3. Five-component internal rotational signature of the *c*-type, *Q*-branch transitions of Conf. 3.

SPCAT program[39] was used with implementing a semirigid rotor model in the Watson-S reduction and I^r representation.[40]

After removing the SPFIT/SPCAT-assigned transitions corresponding to Conf.2 and Conf.3 from the spectrum, we were able to identify the lowest zero-point energy conformer (Conf.1) despite its low μ_b dipole moment value of 0.2 D. A total of 26 *b*-type rotational lines were observed in the measured microwave spectrum and fitted to a root-mean-square deviation of 9.7 kHz. The rotational constants *A*, *B*, and *C* as well as the centrifugal distortion parameters were determined (FIT 1 of Table 2).

Once the pure rotational spectrum was completed for the three conformers (Table 2: FIT 1, FIT 2, and FIT 4 for Conf.1, Conf.2, and Conf.3, respectively), the internal rotations of the two SiH_3 groups could be taken into account, since their *b*-type and *c*-type transitions are split in the experimental spectrum. Figure 2b shows an example of this with the $2_{11} \leftarrow 2_{02}$ and $3_{12} \leftarrow 3_{03}$ transitions of Conf.2 split into quadruplets. These observed splittings are in agreement with our expectations. As stated previously, the predicted geometry of Conf.2 (see Table 1) confirms the presence of two equivalent C_{3v} internal rotors, with C_{2v} symmetry at equilibrium, which leads to the split of four rotational energy levels due to internal motions as explained in detail in ref 41.

Internal Rotation Analysis. Internal rotation spectral analysis requires suitable theoretical models and Hamiltonians in order to reproduce the splitting in the spectra. The *XIAM* program[42] is very convenient for our case of study, since it has already shown its efficiency for treating internal rotation with different values of V_3 potential barriers. This program uses the Combined Axis Method (CAM), where the rotation-torsion Hamiltonian is set up in the rho axis system (RAM), for each top, then converted into the principal axis system (PAM).[43]

The *XIAM* program can be applied to molecules containing two equivalent C_{3v} internal rotors as in the case of dimethyl sulfide (CH_3SCH_3).[44] It can also be used for molecules containing two nonequivalent C_{3v} internal rotors as in the case of ethyl methyl ketone.[45] For TSP, we will use hereafter both of these theoretical approaches, since the two SiH_3 internal rotors are equivalent for Conf.2 and nonequivalent for Conf.3, respectively. No internal rotation signatures, that is, splittings, were observed in the Conf.1 spectra.

In a first step, a theoretical spectrum of Conf.2 between 10 and 11 GHz was predicted with the *XIAM* program, where the pure rotational part in the Hamiltonian was produced using the obtained experimental *A*, *B*, and *C* constants as well as the centrifugal distortion constants from the pure rotation analysis (FIT 2 of Table 2). The starting internal rotation Hamiltonian was derived from ab initio calculations. The V_3 potential barrier heights were estimated to be 320 cm^{-1}, and the F_0 rotational constants of the two SiH_3 groups were fixed to 87 GHz ($F_0 = \frac{\hbar^2}{2I_a}$ where I_a is the moment of inertia). The angles between the internal rotor axes and the principal *a*-, *b*-, and *c*-axes were taken from ab initio results at the MP2/6-311++G(d,p) level (Table 1).

By direct comparison of this calculated spectrum with measured rotational lines as illustrated in Figure 2b, the $2_{11} \leftarrow 2_{02}$ and $3_{12} \leftarrow 3_{03}$ transitions of Conf.2 could be assigned to the S1, S2, S3, and S4 internal rotation components. Identification and fit of all the split lines of Conf.2 were progressively performed by trial and error. Experimental spectroscopic parameters including potential barrier heights for internal rotation (V_{3_1} and V_{3_2}) were finally determined in a global fit of 53 transitions, converging with an rms deviation of 14.7 kHz. Fit 3 of Table 2 summarizes all the obtained rotational constants with our *XIAM* analysis.

The internal rotation analysis process of Conf.3 was slightly different for several reasons. First, the calculated dipole moment components were lying in the *a*- and *c*-axis directions. Therefore, *c*-type transitions were targeted first, since the $-SiH_3$ internal rotational effect is estimated to be larger and more clearly observed in the microwave spectrum. For example, we show in Figure 3 the $3_{22} \leftarrow 3_{12}$ and $4_{23} \leftarrow 4_{13}$ *c*-type, *Q*-branch transitions, where rotational signatures are split into five components, labeled as S1, S2, S3, S4, and S5.

Using an iterative procedure of assignment and fit, we succeeded in identifying 336 transitions for Conf.3, where this set of data contains simultaneously the five different species due to SiH_3 internal rotation motions. The experimental spectroscopic constants are summarized in FIT 5 of Table 3. The barrier heights hindering the internal rotations of SiH_3 tops were determined to be V_{3_1} = 347.78(21) cm^{-1} and V_{3_2} = 360.18(88) cm^{-1}. The illustrated set of data in FIT 5 of Table 2 converged with a root-mean-square deviation of 23 kHz, slightly higher than the estimated experimental accuracy. This is probably due to the presence of several overlapping transitions corresponding to energy levels, which are essentially degenerate to the resolution of the instrument, such as the S1 and S2 species of the $4_{23} \leftarrow 4_{13}$ transition in Figure 3. Similar overlapping of transitions occurs for the S3, S4, and S5 components for almost all the *a*-type, *R*-branch transitions.

DISCUSSION

At the beginning of the study, there were three major aspects that the authors set out to address. These were the

https://dx.doi.org/10.1021/acs.jpca.0c01100
J. Phys. Chem. A 2020, 124, 3825−3835

Table 3. Comparison of Some Similar SiH_3 Internal Rotation Barriers

molecule	formula	V_{3_1}, cm^{-1}	V_{3_2}, cm^{-1}	ref
methylsilane	CH_3SiH_3	595		1
chloromethylsilane	CH_2ClSiH_3	826		8
		892		12
		927		13
fluoromethylsilane	CH_2FSiH_3	717		11
dichloromethylsilane	$CHCl_2SiH_3$	887		8
silyl methyl ether	CH_3OSiH_3	385		14
disilylsulfide	$S(SiH_3)_2$	183	183	15, 16
silylphosphine-d2	SiH_3PD_2	528		17
disilane	H_3SiSiH_3	407	407	18, 19
1,3,5-trisilapentane	$SiH_3CH_2SiH_2CH_2SiH_3$			
	Conf.2	368	368	this work
	Conf.3	348	360	this work

conformational landscape and ordering of the possible TSP conformers, the molecular structure of each observed conformer, and the comparison of the internal rotation barriers of the SiH_3 rotors compared to similar silyl rotor-containing molecules.

Although both Conf.1 and Conf.2 are lower in energy than Conf.3 in our zero-point energy calculations, there were significantly more transitions observed and assigned for Conf.3 than the other two observed species, and the spectra belonging to Conf.3 were, in general, more intense than those of the other species. While the dipole moment of Conf.2 is the largest, if it were the next in energy, given the rotational temperature of the molecular beam source (~1 K), we would expect its spectra to be the most intense. Conf.3, as shown in Figure 2, proves this not to be the case. Furthermore, more transitions were observed for Conf.3 than any other species.

All of these inconsistencies justified revisiting the calculation of the energy landscape at multiple basis sets and theoretical approaches explained in the Quantum Chemical Calculations section. Although the B3LYP method provided correct geometrical structures, this does not reproduce the intensity data observed in the spectra. However, the MP2 method provides both structures and energy orderings in agreement with what is observed experimentally. Furthermore, these calculations become more aligned with the intensity data as the basis set is increased (see Tables S1−S5 of the Supporting Information). These calculations correspond to an energy ordering of C_2 (Conf.1) < C_1 (TG, Conf.3) < C_{2v} (Conf.2). This is an interesting result, as it is in stark contrast to the energy orderings for the conformations found for *n*-pentane, *n*-butylsilane, and 1,5-disilapentane, TSP's closest molecular comparators. This must arise from the elongation of the Si−C bond from that of the C−C bond and the size of a Si atom for which the C_2 and C_1 (TG) structures relieve steric hindrance in comparison to C_{2v} (see Figures 1 and 4). Furthermore, the dipole information calculated at high levels of theory for MP2 (Tables S3−S5) may also provide a clue as to why the C_1 (GG′) structure (if it exists) was not observed as it was in *n*-pentane. The overall dipole moment is less in C_1 (GG′) than that of C_{2v}, and it consists of dipole components in all three axes, most likely lowering the possibility of the observation of these transitions in the beam. We do not have the capability to do experiments outside the beam, so these calculations were provided to aid in future experiments on the TSP species.

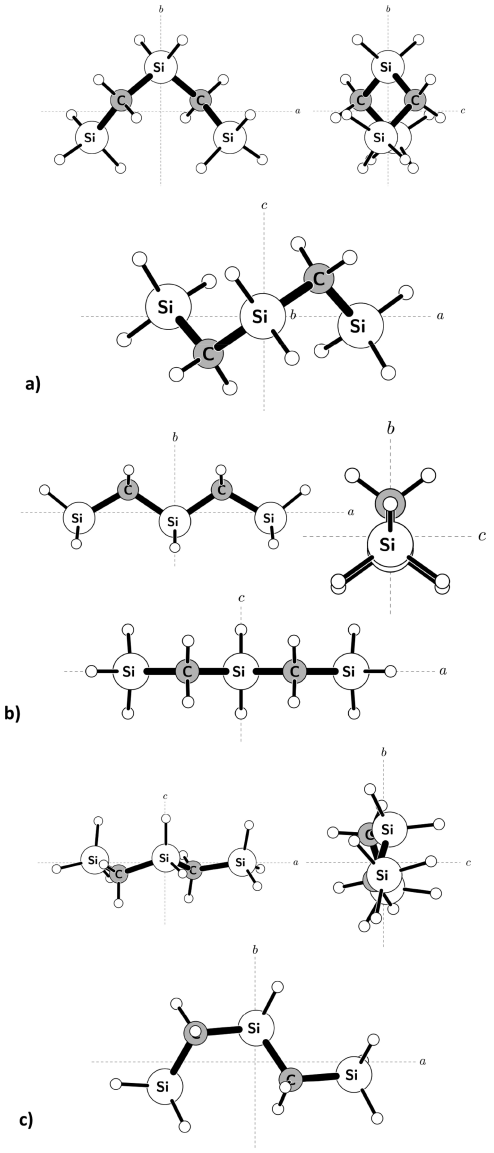

Figure 4. Conf.1 (a), Conf.2 (b), and Conf.3 (c) in the *ab*, *ac*, and *bc* planes. The *b*-axis can be seen as the C_2 axis of symmetry in Conf.1 and Conf.2, while there is no such axis or plane for Conf.3.

There are, however, exceptions that should be considered that could cause this conclusion not to be the case. One explanation for the increase in transitions for Conf.3 is that there are dipole moment components along the *a*- and *c*-axes instead of just one axis, as is the case for Conf.2, providing for more transition types to be leveraged. Transition types themselves follow different rigid rotor patterns that are dependent on the rotational constants themselves and, given a specific frequency range, may favor the observation of more transitions for specific conformers regardless of energy ordering.[46] In this case, Conf.3 does, overall, possess smaller rotational constants than Conf.2, lending credence to this possibility. This has been observed by the authors before for the bromine-containing molecules 2-bromo-1,1,1,2-tetrafluoroethane[47] and 3-bromo-1,1,1,2,2-pentafluoropropane,[48] where more ^{81}Br isotopologue species were observed than the ^{79}Br, due to more transitions simply falling in the spectrometer's

https://dx.doi.org/10.1021/acs.jpca.0c01100
J. Phys. Chem. A 2020, 124, 3825−3835

region. Furthermore, the two inequivalent tops in Conf.3 provide for there to be five components in split transitions instead of the four from the equivalent tops of Conf.2, possibly providing an explanation for the increase in transitions observed. Although any or all of these could certainly rationalize the observation of more spectral lines for Conf.3, the intensity of Conf.3's spectra cannot be ignored with respect to the other conformers, giving way to our earlier conclusion of it being the second in relative energy to Conf.1 for the TSP molecule.

The calculated structures of the conformers observed, compared to the experimentally observed structures, is something that is much more easily achieved. To visualize these comparisons, the quantum-chemical calculated structures of Confs.1−3 were shown in the *ab*, *ac*, and *bc* planes in Figure 4. Although the determined spectroscopic parameters from the experimental spectrum lack any isotopologue information in order to arrive at an experimental substitution structure, there are still some conclusions that can be drawn from the determined parameters. As a starting point, we compared the calculated *A* rotational constants to those experimentally determined to arrive at a percent accuracy for the agreement. Calculated Conf.1 and experimentally determined Conf.1 are ∼2.5% different, Conf.2 is ∼2.2% different, and Conf.3 is ∼2.0% different, with Conf.2 overpredicting *A* and Conf.1 and Conf.3 underpredicting *A* for the experimental structure.

This way of comparing the structures, however, is not very quantitative and provides little insight. Therefore, in the situations where only parent isotopologue spectra are available, a great method for comparison is the second moment method put forward by Bohn.[49] This method takes average contributions to the planar moments from molecular families and establishes average values for their contributions. For instance, the CH_2/CH_3 groups in long-chain alkane molecules average each a contribution of 1.6 uÅ^2 to P_{cc}, due almost primarily to the two H atoms being out of the *ab* plane. Using this method along with some common bond length/bond angle knowledge, the experimental structures can be built up to arrive at the given structures. This has been done in some of the authors' previous work.[33]

To start, then, the authors have reported the planar moments of the calculations and the experimentally determined structures in Tables 1 and 2. Because Conf.2 has the heavy-atom backbone structure effectively all in the *ab* plane, it is best to start there in order to have the best comparisons to Bohn's work and extend to the SiH_2/SiH_3 functional groups. The experimental P_{cc} for Conf.2 is taken to be 12.1 uÅ^2 from FITS 2 and 3. Subtracting Bohn's 1.6 uÅ^2 for each CH_2 group, the remaining value of P_{cc} due to the SiH_2 and SiH_3 groups is 8.9 uÅ^2. An easy approximation for the origin of 1.6 uÅ^2 can be made by assuming a typical C−H bond of 1.09 Å and a H−C−H bond angle of 109.5°. Using trigonometry, each C−H group contributes ∼0.8 uÅ^2. Two, of course, give the contribution of 1.6 uÅ^2 that Bohn has cited as typical. CH_3 has one of the hydrogens in the *ab* plane, so it does not contribute. With this same approach, the typical Si−H bond length of 1.48 Å may be used with the same 109.5° bond angle to arrive at a contribution of 1.46 uÅ^2 for each Si−H unit or 2.92 uÅ^2 for the group (again, assuming the third H is in-plane and does not contribute). There are three SiH_2/SiH_3 units, giving 8.76 uÅ^2, or 0.14 uÅ^2 off the experimental value. Given our approximations and that Bohn's method is set from experimental data from entire families of molecules, this is exceptional agreement.

Conf.1 can be determined similarly to Conf.2 assuming that the calculated structure in Figure 4 is a reasonable approximation for the axis system. Looking at the molecule in the *bc* plane, the contribution to P_{cc} will be very similar to Conf.2, except that there are now large contributions from the carbon atoms themselves being out-of-plane. We will ignore the slight contribution due to the Si atoms being slightly out-of-plane. A typical Si−C bond length is 1.86 Å while, again, it will be assumed the bond angles are 109.5°. With trigonometry and the mass of carbon, each out-of-plane carbon contributes an additional 13.8 uÅ^2 from the Conf.2 result. 12.1 uÅ^2 + 2 × 13.8 uÅ^2 gives 39.7 uÅ^2, overestimating the experimental value of 37.7 uÅ^2 by 2 uÅ^2. This is not as satisfying as the Conf.2 argument, though, because it seems too far away given the experimental accuracy. Another way to look at the structure is to realize that the P_{bb} value of Conf.2 is almost the exact same P_{cc} value contribution for Conf.1 with some extra contribution coming from the Si atoms. The P_{cc} value for Conf.2 is 35.1 uÅ^2, underestimating the experimental value by ∼2.6 uÅ^2, so our original approach is reasonable given our neglect of the Si atom contribution.

Finally, we address the structure of Conf.3 using the Bohn method. Without a large repository of experimental data on which to base contributions, it is difficult to be quantitative. However, a qualitative approach can still be used in making experimental structural determinations for this conformer. As shown in Figure 4 for the *bc* plane, this structure is predicted to be between the extremes of Conf.1 and Conf.2 for the distribution of the mass along the *a*-axis. There will be less influence on the P_{cc} value by the Si and C atoms, but certainly some contribution will come from these, because they now lie outside the *ab* plane. The experimental P_{cc} value for Conf.3 is 19.15 uÅ^2, which is closer to the Conf.2 P_{cc} value than Conf.1 as predicted from the quantum-chemical calculations, demonstrating this qualitative agreement.

Last of all, it is important to contextualize the findings from our observations for the internal rotation parameters determined for each conformer of TSP as well as place these findings within the context of SiH_3 rotors as a whole. Conf.2 and Conf.3 each possessed splitting in the spectra for which an internal rotation barrier was determinable. For Conf.2 with equivalent rotors, this barrier was determined to be 368.46 ± 0.33 cm^{-1}, and, for Conf.3 with inequivalent rotors, the barriers were determined to be 347.78 ± 0.21 and 360.18 ± 0.88 cm^{-1}, respectively. These determined barriers are very reasonable, because the calculated barriers are 320 cm^{-1} for Conf.2 and 320 and 340 cm^{-1} for Conf.3, putting all measured barriers consistently 20−30 cm^{-1} higher than their calculated values (because the higher and lower barriers correlate in Conf.3). The larger barrier in Conf.3 corresponds to the right rotor in Figure 4 in the *ab* plane representation and makes sense to be higher, because the hydrogens of the middle Si atom are pointed toward that silyl group, providing slightly more interference from free rotation than that of the other SiH_3 rotor.

The next question regarding internal rotation to address is was it reasonable that no splitting was observed in Conf.1? This barrier was calculated to be 20 cm^{-1} higher in energy than any other calculated barrier, and all determined experimental barriers were 20−30 cm^{-1} above their prediction. From this standpoint, Conf.1 internal rotation was certainly the least

https://dx.doi.org/10.1021/acs.jpca.0c01100
J. Phys. Chem. A 2020, 124, 3825−3835

likely to be observed, as was stated previously, but now possibly even more unlikely than originally calculated. This is reinforced by the fact that some transitions were already effectively degenerate on the observed internal rotation signatures in the CP-FTMW spectrum.

Finally, it is important to put these experimentally observed barriers into context with similar molecules. To do this, comparisons of some V_3 barriers of similar molecules were presented in Table 3. All of the barriers reported are less than 1000 cm^{-1}. However, there is a trend that, as the hydrogens of the silyl rotor are eclipsing atoms of larger size (fluorines and chlorines) or if the eclipsing hydrogens are closer due to the bond length of the Si−X moiety, then the barrier is higher. It is interesting to note that what would be considered the simple model molecule to this system, methylsilane, is actually almost 200 cm^{-1} above these determined barriers (595 cm^{-1}). However, the barriers determined here are very comparable to disilane (407 cm^{-1}) and silyl methyl ether (385 cm^{-1}). This would imply that having such separation between the two rotors actually relieves steric hindrance and eases rotation. A study of a hexane with terminal silyl rotors would be an excellent test of this hypothesis. This compilation of barriers does show that the experimentally determined barriers of this work are very reasonable and fit nicely into the previous works on silyl rotors.

CONCLUSIONS

The CP-FTMW spectrum of 1,3,5-trisilapentane has been observed and is reported. The observed spectrum contained the lowest three energetic conformers as predicted by ab initio (MP2) quantum-chemical calculations. These conformers are of C_2, C_{2v}, and C_1 symmetry, respectively, with an energy ordering predicted to be $C_2 < C_1$ (TG) $< C_{2v}$, which has been determined to be in agreement with the experimentally observed spectra, but in stark contrast to *n*-pentane and all known silicon *n*-pentane derivatives. The density functional theory (DFT) method, B3LYP, was also utilized and is shown to give a different energy ordering not in agreement with the observed rotational spectra. Internal rotation has been observed in Conf.2 and Conf.3 but not in Conf.1, which is in accordance with the likelihood of observing these signatures from the predicted barrier heights. The conformers' quantum-chemical structures have been determined to be an accurate depiction of the experimental structures based upon the determined experimental planar moments using the method of Bohn. The determined internal rotational barriers are 368.46 ± 0.33 cm^{-1} for Conf.2's equivalent rotors and 347.78 ± 0.21 and 360.18 ± 0.88 cm^{-1} for Conf.3's inequivalent rotors. These have been compared to the same values of similar molecules with silyl rotors and were found to be more comparable to species with less-hindered silyl rotors like disilane than, surprisingly, what may be considered the simplest comparator, methylsilane.

ASSOCIATED CONTENT

Supporting Information

The Supporting Information is available free of charge at https://pubs.acs.org/doi/10.1021/acs.jpca.0c01100.

Energy and structure calculations using multiple basis sets and methods. SPFIT/SPCAT and XIAM output files with quantum number assignments (PDF)

AUTHOR INFORMATION

Corresponding Author

G. S. Grubbs II − *Department of Chemistry, Missouri University of Science and Technology, Rolla, Missouri 65409, United States;* orcid.org/0000-0002-1162-8819; Phone: (573)-341-6281; Email: grubbsg@mst.edu

Authors

Atef Jabri − *Laboratoire Interuniversitaire des Systèmes Atmosphériques, CNRS UMR 7583, Université Paris-Est Créteil & Université de Paris, Institut Pierre Simon Laplace, Créteil F-94010, France*

Frank E. Marshall − *Department of Chemistry, Missouri University of Science and Technology, Rolla, Missouri 65409, United States*

William Raymond Neal Tonks − *Department of Chemistry and Biochemistry, College of Charleston, Charleston, South Carolina 29424, United States*

Reid E. Brenner − *Department of Chemistry, University of Missouri-Kansas City, Kansas City, Missouri 64110, United States*

David J. Gillcrist − *Department of Chemistry, Missouri University of Science and Technology, Rolla, Missouri 65409, United States*

Charles J. Wurrey − *Department of Chemistry, University of Missouri-Kansas City, Kansas City, Missouri 64110, United States*

Isabelle Kleiner − *Laboratoire Interuniversitaire des Systèmes Atmosphériques, CNRS UMR 7583, Université Paris-Est Créteil & Université de Paris, Institut Pierre Simon Laplace, Créteil F-94010, France;* orcid.org/0000-0002-8715-9764

Gamil A. Guirgis − *Department of Chemistry and Biochemistry, College of Charleston, Charleston, South Carolina 29424, United States;* orcid.org/0000-0002-2202-0964

Complete contact information is available at: https://pubs.acs.org/10.1021/acs.jpca.0c01100

Notes

The authors declare no competing financial interest.

ACKNOWLEDGMENTS

This material is based upon work supported by the National Science Foundation under Grant No. CHE-1841346. G.S.G.II acknowledges a Univ. of Missouri Research Board grant for instrument support and the OURE program at Missouri S&T for undergraduate student support. This research is supported in part by a grant to the College of Charleston from the Howard Hughes Medical Institute through the Precollege & Undergraduate Science Education Program. The NMR spectrometer used in this study at the College of Charleston is supported by the National Science Foundation under Grant No. 1429308. The computation for this work was performed on the high-performance computing infrastructure provided by Research Computing Support Services and in part by the National Science Foundation under Grant No. CNS-1429294 at the Univ. of Missouri. In addition, the authors acknowledge the International Symposium on Molecular Spectroscopy (ISMS) and its 75th annual meeting. ISMS has had a tremendous impact on many of our careers, and the work contained herein was first presented at the ISMS conference. This conference was and continues to be one of the best forums for idea exchange and the shaping of careers,

particularly for spectroscopists in their early years. Each member of the authorship wishes to thank all of the stewards, both past, present, and future, who have shaped the conference and continue to build its wonderful legacy.

REFERENCES

(1) Kilb, R. W.; Pierce, L. Microwave Spectrum, Structure, and Internal Barrier of Methyl Silane. *J. Chem. Phys.* **1957**, *27* (1), 108−112.

(2) Dorris, R. E.; Luce, B. C.; Stettner, S. J.; Peebles, R. A.; Peebles, S. A.; Bullard, J. L.; Bunn, J. E.; Guirgis, G. A. Effect of fluorination on methyl internal rotation barriers: Microwave spectra of cyclopropylfluoromethyl silane (c-C3H5SiHFCH3) and cyclopropyldifluoromethyl silane (c-C3H5SiF2CH3). *J. Mol. Spectrosc.* **2015**, *318*, 101−106.

(3) Ocola, E. J.; Laane, J. Internal Rotation of Methylcyclopropane and Related Molecules: Comparison of Experiment and Theory. *J. Phys. Chem. A* **2016**, *120* (37), 7269−78.

(4) Meerts, W. L.; Ozier, I. Internal Rotation in Methyl Silane by Avoided-Crossing Molecular-Beam Spectroscopy. *J. Mol. Spectrosc.* **1982**, *94*, 38−54.

(5) Foellmer, M. D.; Murray, J. M.; Serafin, M. M.; Steber, A. L.; Peebles, R. A.; Peebles, S. A.; Eichenberger, J. L.; Guirgis, G. A.; Wurrey, C. J.; Durig, J. R. Microwave Spectra and Barrier to Internal Rotation in Cyclopropylmethylsilane. *J. Phys. Chem. A* **2009**, *113*, 6077−6082.

(6) Stolwijk, V. M.; van Eijck, B. P. Microwave Spectrum and Barrier to Internal Rotation of 1-Chloro-2-butyne. *J. Mol. Spectrosc.* **1987**, *124*, 92−98.

(7) Gutowsky, H. S.; Stejskal, E. O. The Infrared Spectrum of Disilane. *J. Chem. Phys.* **1954**, *22* (5), 939−943.

(8) Guirgis, G. A.; Panikar, S. S.; El Defrawy, A. M.; Kalasinsky, V. F.; Durig, J. R. Vibrational spectra, r0 structural parameters, barriers to internal rotation, and ab initio calculations of ClCH2SiH3, Cl2CHSiH3, ClCH2SiF3 and Cl2CHSiF3. *J. Mol. Struct.* **2009**, *922* (1−3), 93−102.

(9) Savoca, M.; George, M. A.; Langer, J.; Dopfer, O. Infrared spectrum of the disilane cation (Si2H6+) from Ar-tagging spectroscopy. *Phys. Chem. Chem. Phys.* **2013**, *15* (8), 2774−81.

(10) Pophristic, V.; Goodman, L.; Wu, C. T. Disilane Internal Rotation. *J. Phys. Chem. A* **2001**, *105*, 7454−7459.

(11) Durig, J. R.; Panikar, S. S.; Groner, P.; Nanaie, H.; Bürger, H.; Moritz, P. Microwave Spectrum, r_0 Structure, Dipole Moment, Barrier to Internal Rotation, and Ab Initio Calculations for Fluoromethylsilane. *J. Phys. Chem. A* **2010**, *114*, 4131−4137.

(12) Durig, J. R.; Hawley, C. W. Vibrational assignments and torsional barrier heights of some methylsilylchlorides. *J. Chem. Phys.* **1973**, *59*, 1−14.

(13) Schwendeman, R. H.; Jacobs, G. D. Microwave Spectrum, Structure, Quadrupole Coupling Constants, and Barrier to Internal Rotation of Chloromethylsilane. *J. Chem. Phys.* **1962**, *36* (5), 1251−1257.

(14) LeCroix, C. D.; Curl, R. F.; McKinney, P. M.; Myers, R. J. Microwave spectrum of silyl methyl ether. *J. Mol. Spectrosc.* **1974**, *53* (2), 250−272.

(15) Dössel, K.-F.; Sutter, D. H. The Microwave Spectrum of Disilylsulfide. *Z. Naturforsch., A: Phys. Sci.* **1978**, *33a*, 500−501.

(16) Dössel, K.-F.; Sutter, D. H. Microwave Spectrum of $(SiH_3)_2X$, X = O,S, r_0-Structure, Molecular, Electric Dipole Moment and Barrier to Internal Rotation of Disilylsulfide. *Z. Naturforsch., A: Phys. Sci.* **1978**, *33a*, 1190−1196.

(17) Durig, J. R.; Li, Y. S.; Chen, M. M.; Odom, J. D. Microwave and Raman Spectra, Dipole Moment, Barrier to Internal Rotation, and Vibrational Assignment of Silylphosphine-d_2. *J. Mol. Spectrosc.* **1976**, *59*, 74−85.

(18) Moazzen-Ahmadi, N.; Horneman, V.-M. The experimental determination of the torsional barrier and shape for disilane. *J. Chem. Phys.* **2006**, *124*, 194309.

(19) Lattanzi, F.; Di Lauro, C.; Horneman, V.-M. Torsional splittings in the v_{12}=1 vibrational state of Si_2H_6: analysis of the $\nu_6+\nu_{12}$ and $\nu_9+\nu_{12}$(E) combination bands in the high resolution infrared spectrum. *Mol. Phys.* **2006**, *104*, 1795−1817.

(20) Fournier, J. A.; Bohn, R. K.; Montgomery, J. A., Jr.; Onda, M. Helical C_2 Structure of Perfluoropentane and the C_{2v} Structure of Perfluoropropane. *J. Phys. Chem. A* **2010**, *114*, 1118−1122.

(21) Mirkin, N. G.; Krimm, S. *Ab initio* studies of the conformation dependence of the spectra of stable conformers of *n*-Pentane and *n*-Hexane. *J. Phys. Chem.* **1993**, *97* (51), 13887−13895.

(22) Murata, H.; Matsuura, H.; Ohno, K.; Sato, T. Vibrational spectra, normal vibrations and rotational isomerism of alkylsilanes: Part I. Propylsilane, butylsilane and their Si-perdeuterium compounds. *J. Mol. Struct.* **1979**, *52*, 1−11.

(23) Matsuura, H.; Ohno, K.; Sato, T.; Murata, H. Vibrational spectra, normal vibrations and rotational isomerism of alkylsilanes: Part II. Ethylmethylsilane, diethylsilane, methylpropylsilane and their Si-perdeuterium compounds. *J. Mol. Struct.* **1979**, *52*, 13−26.

(24) Mitzel, N. W.; Smart, B. A.; Blake, A. J.; Robertson, H. E.; Rankin, D. W. H. Conformational Analysis of 1,4-Disilabutane and 1,5-Disilapentane by Combined Application of Gas-Phase Electron Diffraction and *ab Initio* Calculations and the Crystal Structure of 1,5-Disilapentane at Low Temperatures. *J. Phys. Chem.* **1996**, *100* (22), 9339−9347.

(25) Churchill, G. B.; Bohn, R. K. The Substituted Alkyne 3-Heptyne is Eclipsed. *J. Phys. Chem. A* **2007**, *111* (18), 3513−3518.

(26) Mencarelli, P. The Conformational Behavior of N-Pentane: A Molecular Mechanics and Molecular Dynamics Experiment. *J. Chem. Educ.* **1995**, *72* (6), 511.

(27) Salam, A.; Deleuze, M. S. High-Level Theoretical Study of the Conformational Equilibrium of *n*-Pentane. *J. Chem. Phys.* **2002**, *116* (4), 1296−1302.

(28) Knippenberg, S.; Huang, Y. R.; Hajgató, B.; François, J.-P.; Deng, J. K.; Deleuze, M. S. Probing Molecular Conformations in Momentum Space: The Case of *n*-Pentane. *J. Chem. Phys.* **2007**, *127* (17), 174306.

(29) Balabin, R. M. Enthalpy Difference between Conformations of Normal Alkanes: Raman Spectroscopy Study of *n*-Pentane and *n*-Butane. *J. Phys. Chem. A* **2009**, *113* (6), 1012−1019.

(30) LaPlante, A. J.; Stidham, H. D.; Guirgis, G. A.; Dukes, H. W. Vibrational spectra, ab initio calculations, and assignments of the fundamentals of the C_{2v} conformer of *n*-pentane. *J. Mol. Struct.* **2012**, *1023*, 170−175.

(31) Stidham, H. D.; LaPlante, A. J.; Oh, J.-J.; Obenchain, D. A.; Peebles, S. A.; Peebles, R. A.; Wurrey, C. J.; Marrow, E.; Guirgis, G. A. Microwave and vibrational spectra, ab initio calculations, conformational stabilities and assignments of the fundamentals of the C_s conformer of *n*-butylsilane. *J. Mol. Struct.* **2011**, *1003*, 31−40.

(32) Gordy, W.; Cook, R. L. *Microwave Molecular Spectra; Techniques of Chemistry Vol. XVIII,* 3rd ed.; Wiley: New York, 1984.

(33) Marshall, F. E.; Gillcrist, D. J.; Persinger, T. D.; Jaeger, S.; Hurley, C. C.; Shreve, N. E.; Moon, N.; Grubbs, G. S., II The CP-FTMW Spectrum of Bromoperfluoroacetone. *J. Mol. Spectrosc.* **2016**, *328*, 59−66.

(34) Marshall, F. E.; Neill, J. L.; Muckle, M. T.; Pate, B. H.; Kisiel, Z.; Grubbs, G. S., II Observation of $^{36}ArH^{35}Cl$, $^{38}ArH^{35}Cl$ and $^{38}ArH^{37}Cl$ in Natural Abundance using CP-FTMW Spectroscopy. *J. Mol. Spectrosc.* **2018**, *344*, 34−38.

(35) Marshall, F. E.; Dorris, R.; Peebles, S. A.; Peebles, R. A.; Grubbs, G. S., II The microwave spectra and structure of Ar-1,3-difluorobenzene. *J. Phys. Chem. A* **2018**, *122*, 7385−7390.

(36) Sedo, G.; Marshall, F. E.; Grubbs, G. S. Rotational spectra of the low energy conformers observed in the (1R)-(−)-myrtenol monomer. *J. Mol. Spectrosc.* **2019**, *356*, 32−36.

(37) Frisch, M. J.; Trucks, G. W.; Schlegel, H. B.; Scuseria, G. E.; Robb, M. A.; Cheeseman, J. R.; Scalmani, G.; Barone, V.; Mennucci, B.; Petersson, G. A.; et al. *Gaussian 09,* Rev. A.1; Gaussian, Inc.: Wallingford, CT, 2009.

https://dx.doi.org/10.1021/acs.jpca.0c01100
J. Phys. Chem. A 2020, 124, 3825−3835

(38) Frisch, M. J.; Trucks, G. W.; Schlegel, H. B.; Scuseria, G. E.; Robb, M. A.; Cheeseman, J. R.; Scalmani, G.; Barone, V.; Petersson, G. A.; Nakatsuji, H.; et al. *Gaussian 16,* Rev. A.03; Gaussian, Inc.: Wallingford, CT, 2016.
(39) Pickett, H. M. The Fitting and Prediction of Vibration-Rotation Spectra with Spin Interactions. *J. Mol. Spectrosc.* **1991**, *148*, 371−377.
(40) Watson, J. K. G. *Vibrational Spectra and Structure;* Elsevier: Amsterdam, 1977; Vol. *6*, p 1.
(41) Ilyushin, V. V.; Hougen, J. T. A fitting program for molecules with two equivalent methyl tops and C_{2v} point-group symmetry at equilibrium: Application to existing microwave, millimeter, and submillimeter wave measurements of acetone. *J. Mol. Spectrosc.* **2013**, *289*, 41−49.
(42) Hartwig, H.; Dreizler, H. The Microwave Spectrum of trans-2,3-Dimethyloxirane in Torsional Excited States. *Z. Naturforsch., A: Phys. Sci.* **1996**, *51*, 923−932.
(43) Kleiner, I. Asymmetric-top molecules containing one methyl-like internal rotor: Methods and codes for fitting and predicting spectra. *J. Mol. Spectrosc.* **2010**, *260* (1), 1−18.
(44) Jabri, A.; Van, V.; Nguyen, H. V. L.; Mouhib, H.; Tchana, F. K.; Manceron, L.; Stahl, W.; Kleiner, I. Laboratory microwave, millimeter wave and far-infrared spectraof dimethyl sulfide. *Astron. Astrophys.* **2016**, *589*, A127.
(45) Nguyen, H. V. L.; Van, V.; Stahl, W.; Kleiner, I. The effects of two internal rotations in the microwave spectrum of ethyl methyl ketone. *J. Chem. Phys.* **2014**, *140*, 214303.
(46) Cooke, S. A.; Ohring, P. Decoding Pure Rotational Molecular Spectra for Asymmetric Molecules. *J. Spectrosc.* **2013**, *2013*, 698392.
(47) Isert, J. E.; Marshall, F. E.; Bailey, W. C.; Grubbs, G. S. Dipole forbidden, nuclear electric quadrupole allowed transitions and chirality: the broadband microwave spectrum and structure of 2-bromo-1,1,1,2-tetrafluoroethane. *J. Mol. Struct.* **2020**, *1216*, 128277.
(48) Marshall, F. E.; Moon, N.; Persinger, T. D.; Gillcrist, D. J.; Shreve, N. E.; Bailey, W. C.; Grubbs, G. S., II High Resolution Spectroscopy Near the Continuum Limit: The Microwave Spectrum of trans-3-Bromo-1,1,1,2,2-pentafluoropropane. *Mol. Phys.* **2019**, *117* (9−12), 1351−1359.
(49) Bohn, R. K.; Montgomery, J. A., Jr.; Michels, H. H.; Fournier, J. A. Second moments and rotational spectroscopy. *J. Mol. Spectrosc.* **2016**, *325*, 42−49.

https://dx.doi.org/10.1021/acs.jpca.0c01100
J. Phys. Chem. A 2020, 124, 3825−3835